Bi-allelic LAMP3 variants in childhood interstitial lung disease: a surfactant-related disease

Camille Louvrier,[a,b,l,*] Tifenn Desroziers,[a,l] Yohan Soreze,[a,c] Martha Delgado Rodriguez,[a] Lucie Thomas,[a] Valérie Nau,[b] Florence Dastot-Le Moal,[b] Jonathan A. Bernstein,[d] F. Sessions Cole,[e] Markus Damme,[f] Anthony Fischer,[g] Matthias Griese,[h] Daniel Hinds,[g] Laura Keehan,[d] Carlos Milla,[d] Hadhud Mohammad,[i] Jonathan Rips,[i] Jennifer A. Wambach,[e] Daniel J. Wegner,[e] Serge Amselem,[a,b] Marie Legendre,[a,b] Irina Giurgea,[a,b] Sonia Athina Karabina,[a] Oded Breuer,[i] Aurore Coulomb l'Herminé,[j] and Nadia Nathan[a,k]

[a]Sorbonne University, Inserm UMR_S933 Laboratory of Childhood Genetic Diseases, Armand Trousseau Hospital, Paris, France
[b]Assistance Publique Hôpitaux de Paris, Medical Genetics Department, Armand Trousseau Hospital, Paris, France
[c]Assistance Publique Hôpitaux de Paris, Intensive Care Unit, Armand Trousseau Hospital, Paris, France
[d]Department of Pediatrics, School of Medicine, Stanford University, Stanford, CA, USA
[e]Edward Mallinckrodt Department of Pediatrics, Washington University in St. Louis School of Medicine, St. Louis, MO, USA
[f]Christian-Albrechts-University Kiel, Biochemical Institute, Kiel, Germany
[g]Department of Pediatrics, University of Iowa, Iowa City, IA, USA
[h]Department of Pediatric Pneumology, Dr von Hauner Children's Hospital, Ludwig-Maximilians-University, German Center for Lung Research, Munich, Germany
[i]Hadassah Hebrew University Medical Center, Jerusalem, Israel
[j]Assistance Publique Hôpitaux de Paris, Pathology Department, Sorbonne University, Armand Trousseau Hospital, Paris, France
[k]Assistance Publique Hôpitaux de Paris, Pediatric Pulmonology Department, Reference Centre for Rare Lung Diseases (RespiRare), Armand Trousseau Hospital, Paris, France

eBioMedicine
2025;113: 105626
Published Online xxx
https://doi.org/10.1016/j.ebiom.2025.105626

Summary

Background *LAMP3* encodes a lysosomal membrane protein associated with lamellar bodies and has recently been proposed as a candidate gene for childhood interstitial lung diseases (chILD). Here, we identified two *LAMP3* variants in a proband with chILD and performed functional validation of these variants as well as the previously reported variants to demonstrate the role of LAMP3 in pathology.

Methods *LAMP3* variants were identified by exome sequencing. *Ex vivo* studies included mRNA analysis from nasal brushing and lung tissue and immunohistochemistry from lung biopsy. *In vitro* functional analyses in the A549 cell line included immunofluorescence staining and expression analysis of LAMP3. Interactions between LAMP3 and the surfactant protein (SP)-B and SP-C were evaluated by co-immunoprecipitation.

Findings Two heterozygous *LAMP3* variants (Y302Qfs*2 and T268M) were identified in a 15 year old boy with chILD. *LAMP3* mRNA revealed that the frameshift variant resulted in nonsense-mediated mRNA decay. Reduced LAMP3 expression was confirmed in the patient's lung tissue. Functional studies of the T268M and the previously reported G288R variant revealed reduced levels of the mutant proteins. In addition, impaired N-glycosylation and protein instability were demonstrated with the T268M variant. Finally, we provided evidence for an interaction between LAMP3 and SP-B and SP-C, revealing a direct link between LAMP3 and surfactant metabolism.

Interpretation *LAMP3* bi-allelic variants leading to LAMP3 dysfunction emerges as a cause of chILD associated with a heterogeneous phenotype that remains to be further defined. The close links between LAMP3 and surfactant metabolism could explain the pathophysiology of this genetic disease.

Funding No specific funding.

Keywords: Childhood interstitial lung diseases; Surfactant; LAMP3; Lung fibrosis

*Corresponding author. Medical Genetics Department, Armand Trousseau Hospital, 26 avenue du Dr Arnold Netter, Paris, 75012, France.
E-mail address: camille.louvrier@aphp.fr (C. Louvrier).
[l]Both authors contributed equally.

Research in context

Evidence before this study

Childhood interstitial lung disease (chILD) is a heterogeneous group of rare and devastating respiratory disorders. Abnormalities in surfactant-related genes are the most common cause of chILD, but the aetiology of chILD remains unclassified in up to 30% of affected individuals. Recently, *LAMP3* has been proposed as a candidate gene for chILD.

Added value of this study

This study identified *LAMP3* bi-allelic variants leading to LAMP3 dysfunction as a cause of chILD. It provides an *in vitro* functional characterisation of *LAMP3* variants and highlights that LAMP3 protein function is closely linked to surfactant metabolism.

Implications of all the available evidence

LAMP3 dysfunction emerges as a molecular cause of chILD, affecting surfactant metabolism. This study supports the inclusion of *LAMP3* sequencing in the workup of chILD and adult ILD.

Introduction

Childhood interstitial lung diseases (chILD) encompass a wide, heterogeneous group of rare and severe respiratory disorders that are characterised by an early childhood onset with progressive chronic respiratory disease, with high morbidity and mortality.[1,2] The pathophysiology of chILD is incompletely understood and probably involves diverse molecular and environmental mechanisms that lead to inflammatory and fibrotic alterations of the lung parenchyma.[3] Of all chILD aetiologies, molecular abnormalities in surfactant-related genes are among the most common (≈20%) causes.[4–6] However, for up to 30% of affected individuals, the aetiology of chILD remains unclassified.[6]

In 2020, a segregation study performed in Airedale Terrier (AT) dogs identified a homozygous missense variant c.1159G>A, p.(Glu387Lys) (E387K) in *LAMP3* (Lysosomal-associated membrane protein 3) in 25 affected puppies from the same pedigree who presented with fatal neonatal respiratory distress.[7] Although no functional study was performed, the AT dog's lamellar bodies were abnormal, and this study suggested *LAMP3* as a strong candidate gene for surfactant disorders. These results were further supported in 2021 by a mouse model that showed that LAMP3 deficiency affected surfactant homoeostasis in *Lamp3* KO mice.[8] Notably, the mice are mildly affected with no premature death. Recently, an Israeli team identified by whole exome sequencing (ES) the c.862G>A, p.(Gly288Arg) (G288R) *LAMP3* homozygous missense variant in seven individuals with ILD in a large consanguineous family.[9] However, no functional study has been carried out to assess the pathogenicity of G288R. In addition; three patients from two families have very recently been reported at a medical meeting, they all exhibited neonatal respiratory distress, and a comprehensive phenotypic characterisation of these cases is currently underway.[10]

LAMP proteins are a family of highly glycosylated lysosomal proteins. They comprise approximately half of the proteins of the lysosomal membrane, forming a glycoprotein coat on the inside of the lysosomal membrane. The major LAMP family members are LAMP1 and LAMP2, which are ubiquitously and abundantly expressed in lysosomes but also in late endosomes and mature phagosomes[11,12] and are involved in maintaining lysosomal integrity.[12] More recently identified, LAMP3, also known as DC-LAMP or CD208, was originally described to be expressed in mature dendritic cells (DCs). Recently, it has been shown that LAMP3 is also highly expressed in human lung tissue and, more specifically, in type 2 alveolar epithelial cells (AEC2).[13,14] In AEC2 cells, LAMP3 localises to the limiting membrane of lamellar bodies (LBs), in a similar pattern (ring-like structures) as the surfactant transporter ATP-binding cassette family A, member 3 (ABCA3).[15] Although the exact function of LAMP3 in human AEC2 cells remains elusive, the subcellular localisation of LAMP3 suggests a likely role in pulmonary surfactant processing and/or trafficking.[13] Similar to other LAMP members, LAMP3 is composed of a N-terminal signal peptide, a LAMP domain with two conserved disulfide bonds, followed by a transmembrane helix and ending with a cytoplasmic C-terminal tail. LAMP3 is highly N-glycosylated with seven total N-glycosylation sites throughout its different domains.[12]

Following the detection of two heterozygous *LAMP3* variants in a patient with chILD from the RespiRare network, we report here the functional consequences of these newly identified variants as well as of the previously published variants in humans and in AT dogs.

Methods

Ethics

Clinical information was collected through the proband's medical file in a legally authorised database (CNIL N°681248). Written informed consent was obtained from the proband's parents for genetic tests and data sharing according to French law and the principles of the Declaration of Helsinki. The study is part of the chILD genetic project approved by the ethical authorities (Comité de protection des personnes n°20130604).

DNA sequencing

Genomic DNA was extracted from peripheral blood leukocytes of the proband and his parents. Exome sequencing (ES) was performed using the MedExome SeqCap EZ kit (Roche). Sequencing was performed on a NextSeq500 (Illumina) platform according to the manufacturer's instructions. Sequence reads in fastq format were aligned to the reference human genome (hg19) with BWA. Variant calling was performed with GATK, VarScan, Bcftools, Vardict and Pindel. Variant calls in a vcf format were annotated through SNPEff and SnpSift. The following filters were then applied to identify rare, predicted pathogenic variants: variant allele fraction (VAF) above 0.10, minor allele frequency (gnomAD v2.1.1) less than 1%, less than three occurrences in the local laboratory database (n = 164); the analysis of null variants (nonsense, frameshift, splice donor, or splice acceptor variants) as a first step and then of non-synonymous (i.e., missense variants and in-frame insertions or deletions) and splice region variants. The stepwise elimination process is shown in Supplemental Figure S1. The results obtained by ES were confirmed by Sanger sequencing. *LAMP3* exons 3 and 4 were amplified by polymerase chain reaction (PCR) and analysed by Sanger sequencing using a BigDye Terminator sequencing kit (Applied Biosystems) on an ABI 3730XL automated capillary DNA sequencer (Applied Biosystems). Sequences were compared to the *LAMP3* reference sequence (NM_014398).

Lung tissue staining

Lung biopsies from control and proband were analysed by haematoxylin and eosin stain (HES) and by immunohistochemistry using anti-CD208 antibody (Cell Signalling Technology Cat# 47778, RRID: AB_3107069) at dilution 1/200 anti SP-B antibody (Abcam ab271345) at dilution 1/1000, anti pro-SP-B (Abcam ab231551) at dilution 1/1000, anti-SP-C antibody (Santa Cruz Biotechnology Cat# sc-13979, RRID: AB_2185502) at dilution 1/100 and anti pro-SP-C (Abcam Cat# ab90716, RRID: AB_10674024) at dilution 1/1000, on a Leica Bond Platform.

Plasmids constructs

LAMP3 (NM_014398.4) cDNA vector pCMV3_LAMP3 (with C-terminal HA-tag) was purchased from Sinobiological (#HG10527-CY). Site directed mutagenesis was performed on pCMV3_LAMP3 with high fidelity polymerase (Q5 HF NEB) to generate mutant plasmids pLAMP3_E375K, pLAMP3_T268M, pLAMP3_G288R, and pLAMP3_N266A.

Cell culture and transfection

Airway epithelial cells extracted from the proband's nasal brushing were seeded in collagen I coated flask and cultured in PneumaCult-Exp Plus medium (Stem Cell) supplemented with 5% FBS and 10 μM ROCK inhibitor (Y27632, SIGMA). At confluence, cells were seeded in collagen IV-coated transwell inserts (Costar) in the same EXP Plus-FBS-ROCK medium. When confluence was reached, the supernatant was removed from the apical surface and replaced in the basal chamber by PneumaCult-ALI medium (StemCell) in order to expose cells to an air-liquid interface that promotes *in vitro* differentiation over 1 month interval.

A549 cells (CCL-185 ATCC) were cultured on DMEM 1 g/l (Thermo Fisher) glucose complemented with 10% foetal bovine serum (FBS) and 1% penicillin/streptomycin. Cells were transfected with 3 μL of FuGene (Promega) per 1 μg of plasmid in OptiMEM (Thermo Fisher) according to manufacturer's protocol.

RNA extraction and reverse transcription

RNA from nasal cell culture was extracted using the RNeasy Mini Kit (Qiagen) including a DNAse step according to the manufacturer's protocol. RNA from lung biopsy was extracted using the Maxwell RSC simply RNA tissue Kit on a Maxwell RSC instrument (Promega) according to the manufacturer's protocol with an initial stage of manual grinding of lung tissue on dry ice. cDNA from RNA samples were obtained using Transcriptor High Fidelity cDNA Synthesis Kit (Roche). PCR was assessed on cDNA with GoTaq green polymerase (Promega) and the following primers: 5′-ACAGCTGATTGTTCAAGACAAGG-3′ (exon 2, forward) and 5′-CAGGTGGGCTGACAACTGGAG-3′ (exon 5, reverse). Amplicons were controlled by electrophoresis and then sequenced by Sanger sequencing using a BigDye Terminator sequencing kit (Applied Biosystems) on an ABI 3730XL automated capillary DNA sequencer (Applied Biosystems).

Subcellular localisation analysis

Following 48 h after transfection, A549 cells were fixed with 4% paraformaldehyde for 15 min, incubated with NH_4Cl 50 mM for 10 min, permeabilized with Perm/Wash 1× (BD Bioscience) for 15 min, blocked with BSA 2% for 1 h, incubated for 2 h with an anti-HA Monoclonal Antibody (2-2.2.14) DyLight 488 (Thermo Fisher Cat# 26183-D488, RRID: AB_2533051) at 1/200 dilution and mounted with ProLong Gold Antifade Reagent with DAPI (Cell Signalling).

Cycloheximide (CHX) protein stability assay

Following 24 h after transfection, A549 cells were treated with 100 μg/ml cycloheximide (CHX, Merck) at different times. The expression of proteins from soluble lysate was detected by Western blot.

Protein extraction

Cells were harvested 48 h after transfection or after treatment and lysed with RIPA 1× (RIPA 5×: 250 mM Tris HCl pH 7.5, 750 mM NaCl, 5% Triton, 5% Sodium Deoxycholate) and cOmplete protease inhibitor 1×

(Roche). Soluble lysate was separated from total lysate by centrifugation for 10 min at 20,780 g. Cell pellet was discarded and supernatant was diluted with Laemmli 2× DTT (4×: 250 mM Tris pH 6.8, 9% SDS, 200 mM DTT, 40% Glycerol, Bromophenol blue).

Immunoprecipitation

Soluble cell lysates (500 µL) were incubated with anti-HA Magnetic beads (IP HA) (ThermoFisher 88836) for 3 h at room temperature (RT) with end-over-end rotation according to the manufacturer's protocol. After five washes with tris buffered saline solution, samples were eluted by heating for 10 min at 95 °C with 30 µL of Laemmli 4× DTT.

Western blot analysis

Proteins from soluble cell lysates were loaded under reducing conditions onto SDS-PAGE gels and transferred after electrophoresis on nitrocellulose membrane by semi-liquid transfer (TransBlot, BioRad). Membranes were blocked in 5% w/v milk PBS 0.1% Tween-20 for 1 h at RT and incubated overnight with primary antibodies diluted in blocking buffer: 1/1500 anti-HA HRP (Roche Cat# 12013819001, RRID: AB_390917), 1/1500 anti-FLAG HRP (Sigma–Aldrich Cat# A8592, RRID: AB_439702), 1/50 anti-proSP-B rabbit (Abcam ab231551), or 1/1500 anti-α tubulin HRP (Cell signalling Technology 9099 S) 1/1500 GAPDH HRP (Cell Signalling Technology Cat# 8884, RRID: AB_11129865). The anti-rabbit HRP secondary antibody was incubated for 1 h at RT at dilution 1/5000 (Sigma–Aldrich Cat# A0545, RRID: AB_257896). Proteins were detected with Amersham ECL Select Western-Blotting Detection Reagent (GE Healthcare) according to the manufacturer's recommendations.

Statistics

Signals from Western blot were quantified with Image J tool and Student's unpaired t-test were performed with Graphpad Prism 10.0 software. Data are representative of 3 independent experiments. A p-value ≤ 0.05 was considered significant.

Role of funders

There was no external funding for this study.

Results

Proband

The proband, a 15-year-old boy born to North African distant consanguineous parents, had no neonatal respiratory distress but presented with a cough and dyspnoea on exertion at the age of 9 years, which led to the diagnosis of chILD. He also presented with 21-hydroxylase deficiency requiring a life-long oral supplementation with glucocorticoids (15 mg per day), with growth retardation, micropenis, bilateral cryptorchidism, Arnold Chiari type I compressive malformation which was repaired at the age of three years, and mild neurodevelopmental delay. High-resolution chest CT-scan showed heterogeneous lesions of ILD, including ground-glass opacities, reticulations and parenchymal distortion consistent with early lung fibrosis (Fig. 1a). Exhaustive workup was performed for inflammatory and auto-immune markers with iterative negative results, and targeted next generation sequencing for surfactant-related genes (*ABCA3, NKX2-1, SFTPA1, SFTPA2, SFTPB, SFTPC*) as well as *COPA, CSF2RA, CSF2RB, MARS1,* and *STING1* was non-diagnostic. Environmental ILD are rare in childhood, but a systematic chILD workup has been conducted and no exposures have been identified. Furthermore, the patient has relocated from one city to another, with no observed improvement in their lung disease. The administration of hydroxychloroquine and azithromycin did not result in any clinical or functional improvement. Corticosteroids pulses have been the only treatment to demonstrate a positive impact on the patient's lung status, leading to the discontinuation of oxygen therapy after a year.

To identify the molecular aetiology of chILD in the proband, exome sequencing was performed and revealed two heterozygous variants, the c.904_908del, p.(Tyr302Glnfs*2) (Y302Qfs*2) frameshift variant and the c.803C>T, p.(Thr268Met) (T268M) missense variant in *LAMP3* (Fig. 1b and 2a, Supplemental Figure S1). Each parent was heterozygous for one of the two *LAMP3* variants. Both *LAMP3* variants are reported in the gnomAD database (v.4.1.0) at very low minor allele frequencies (1.3^{E}-4 and 6.1^{E}-5, respectively). The frameshift variant leads to a premature stop codon in the fourth of 6 exons and is therefore expected to result in degradation of the transcripts through nonsense-mediated mRNA decay (NMD). To confirm this hypothesis, Sanger sequencing of the *LAMP3* transcripts isolated from the proband's lung biopsy and nasal epithelial cells revealed a reduction and an absence of the transcripts carrying the c.904_908del variant, respectively (Fig. 1b). The missense variant T268M is predicted as pathogenic according to the Combined Annotation Dependent Depletion score (CADD-score = 26.2). Thr268 is located in the LAMP domain of the protein, within a residue conserved in mammals as well as among three other members of the LAMP family (Fig. 2b–d), therefore suggesting that amino-acid substitutions at this position could be detrimental to LAMP3 function. Interestingly, T268M is near the G288R variant that has been reported in a large consanguineous family with lung disease (Fig. 2a and b).[9]

Finally, the lung biopsy performed at the age 14 years showed thickened alveolar walls with fibrosis, macrophages accumulation in alveolus, enlarged distal airways and microcysts lined by hyperplastic alveolar epithelial cells. Some degree of lymphocytic inflammation was

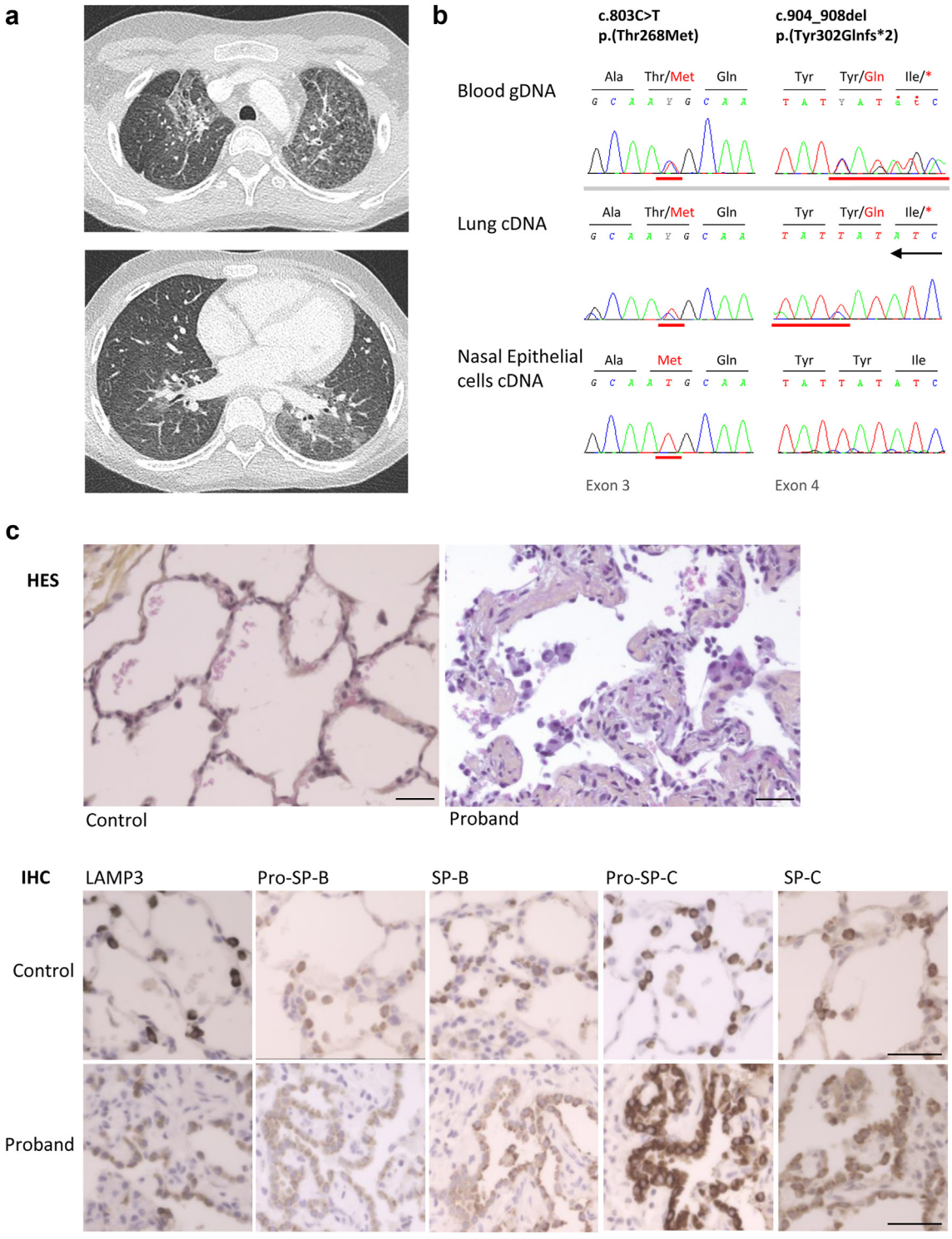

Fig. 1: **Patient**. **(a)** High-resolution computed tomography (CT) scans of the proband carrying bi-allelic *LAMP3* variants characterised by ground glass opacities, reticulations, and parenchymal distortion. **(b)** Sanger electrophoregrams showing the *LAMP3* variants from the proband's blood gDNA, lung, and nasal epithelial cells cDNA. The black arrow below the right electrophoregram of the lung cDNA indicates the reading direction of the sequence. **(c)** Histological analyses of proband and control lung biopsies: haematoxylin and eosin staining (HES) and LAMP3, pro-surfactant protein (SP)-b, SP-B, pro-SP-C, and SP-C immunohistochemistry (IHC). HES revealed septal thickening with hyperplastic alveolar

also observed (Fig. 1c). LAMP3 immunostaining revealed a drastic reduction of LAMP3 expression in the lung from the proband compared to the control (Fig. 1c). The surfactant proteins (SP) SP-B and SP-C were also examined in their immature (proSP-B, proSP-C) and mature forms, and a slight reduction in proSP-B and SP-B immunostaining was observed in the proband's lung biopsy. The marked increase in proSP-C-positive cells may not be indicative of an increase in proSP-C, but rather a reflection of the type 2 alveolar cell hyperplasia (Fig. 1c).

Subcellular localisation and protein expression of LAMP3 mutant proteins

In order to investigate the subcellular localisation of LAMP3, we transiently overexpressed HA-tagged LAMP3 in the A549 cell line in its native form (WT) or mutated forms T268M, G288R, and E375K (corresponding to the human equivalent of the E387K variant in AT dogs). LAMP3 stained ring-like structures with heterogeneous sizes inside the cells in all conditions (WT, T268M, G288R, and E375K), suggesting that the variants did not affect LAMP3 localisation, vesicles size, or cellular trafficking (Fig. 3).

To better understand the impact of the missense variants on the protein structure, an *in silico* analysis was performed using the prediction tool PremPS[16] which uses the protein's three-dimensional conformation (PDB: 4AKM) to predict the impact of missense variants on protein stability. T268M was predicted to be highly destabilising with changes in unfolding Gibbs free energy (ΔΔG) of 1.0 kcal/mol. This missense variant also predicted to drastically change the intra-molecular interactions of the residues compared to the WT (Fig. 4a). G288R and E375K were also predicted to decrease protein stability but to a lesser extent (ΔΔG 0.80 and 0.41 kcal/mol respectively). To confirm these results, LAMP3 protein expression was then assessed in A549 cells after transient overexpression of recombinant LAMP3-HA proteins (WT, T268M, G288R, and E375K) and analysed by Western blot. A major band was observed at about 60 kDa for the WT, the G288R, and the E375K mutants. For the proband's variant T268M, the band was slightly lower (at approximately 57 kDa). Moreover, protein expression for the T268M and the G288R variants were significantly reduced compared to WT, confirming a destabilising effect of these variants on LAMP3. Conversely, the canine variant E375K did not seem to affect protein expression (Fig. 4b). To further demonstrate *in vitro* the destabilising effect of the proband's variant T268M on LAMP3, cycloheximide assay (protein synthesis blocker) was used to determine the half-life of the WT and the mutant protein. The experimental results revealed a shorter half-life of LAMP3 T268M than that of its WT counterpart (1.8 vs 6 h) (Supplemental Figure S2).

N-glycosylation of LAMP3

As a lower-than-expected band was observed for LAMP3 T268M on immunoblot (Fig. 4b), we hypothesised that the T268M variant might impair post-translational modifications of the protein. Indeed, one of the N-glycosylation sites of LAMP3, the asparagine in position 266 (N266) is located near the threonine 268 (Fig. 2). To test this hypothesis, we performed site-directed mutagenesis of *LAMP3* to replace the amino acid N266 with a non-N-glycosylated residue, an alanine. We observed by Western blot, that the N266A negative control of glycosylation band was similar to the band previously observed for the T268M variant, confirming that the T268M variant affects the N-glycosylation of LAMP3 (Fig. 4c). To confirm this result, the protein lysates were then treated with Endo H and PNGase F to remove N-linked glycosylation. After enzymatic treatment, two main bands at approximately 45–46 kDa were obtained in all conditions (WT, T268M, N266A) for both Endo H and PNGase F treatments (Fig. 4c), therefore confirming that the missense variant T268M disturbs the N-glycosylation of the asparagine 266.

LAMP3 and surfactant protein C and protein B interactions

To investigate the links between LAMP3 and surfactant proteins in LBs, we transiently co-expressed LAMP3 with SP-C or SP-B in A549 cell lines and immunoprecipitated LAMP3-HA (IP HA) after protein extractions. We observed by Western blot that the LAMP3 WT or T268M co-immunoprecipitated with proSP-C (Fig. 5a). In addition, the uncleaved immature form of SP-C (proSP-C) was detected to a greater extent following immunoprecipitation of LAMP3 T268M than following immunoprecipitation of LAMP3 WT. The same experiment was also performed with SP-B and similar results were observed for proSP-B (Fig. 5b), indicating that LAMP3 is involved in surfactant protein metabolism, through at least the interaction with SP-B and SP-C, and that LAMP3 abnormalities may be associated with an alteration in surfactant protein homoeostasis.

Discussion

This study supports the hypothesis that *LAMP3* dysfunction is a cause of chILD and provides an *in vitro*

cells and subpleural microcysts, as well as inflammatory interstitial thickening with the presence of lymphocytes. LAMP3 staining revealed a marked lower protein expression for the proband compared to control. Pro-SP-B and SP-B cytoplasmic staining was also slightly reduced in the proband compared to the control. The marked increase of the proSP-C positive cells confirmed type 2 alveolar cell hyperplasia. Scale bar corresponds to 50 μm.

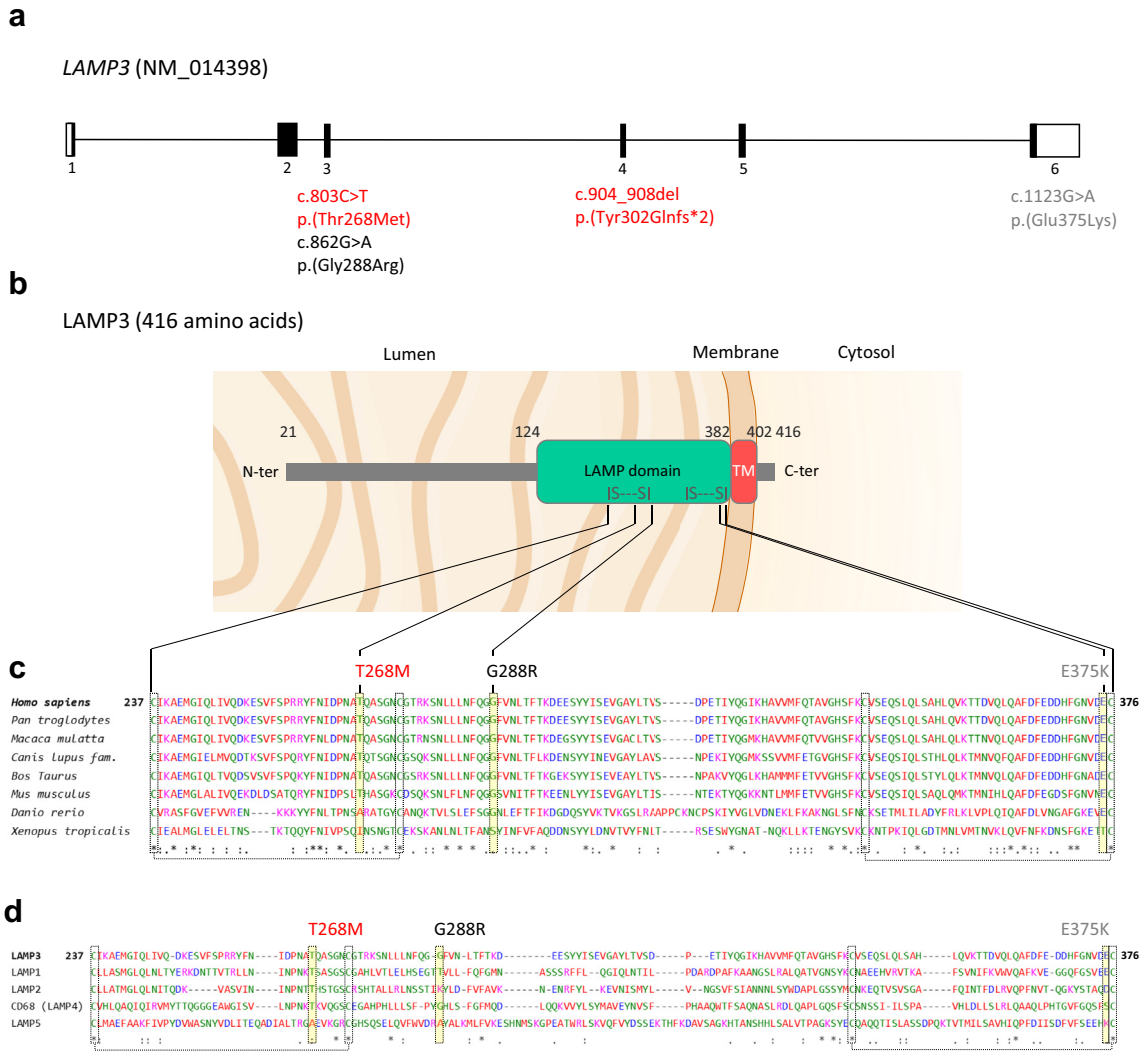

Fig. 2: **LAMP3 gene and protein structure**. **(a)** LAMP3 gene representation with the untranslated exonic region (white box) and the six coding exonic regions (black box). Localisation of the proband's variants in red, the recently reported variant in a family with interstitial lung disease in black and the human equivalent of the canine variation in grey. **(b)** Schematic representation of LAMP3 protein in a lamellar body without its signal peptide (amino acids 1–20). The LAMP (lysosomal-associated membrane protein) domain with disulfide bonds (green) and the transmembrane domain (TM, red) are shown. **(c and d)** Evolutionary conservation of LAMP3 protein across species **(c)**, and in other members of the LAMP family of proteins **(d)**, with a focus on the LAMP domain (237–376 amino acids) and localisation of the amino acids T268, G288, and E375.

functional characterisation of *LAMP3* variants. It also highlights that LAMP3 protein function is closely linked to surfactant metabolism.

The recent findings that a homozygous missense variant of *LAMP3* in the AT dog (E387K corresponding to E375K in human) leads to a fatal neonatal form of respiratory distress and abnormal lamellar bodies have suggested that *LAMP3* could be a candidate gene for surfactant dysfunction in humans.[7] More recently, a study of *Lamp3*$^{-/-}$ mice revealed that these mice surprisingly developed normally and did not display any signs of lung pathology.[8] Nevertheless, surfactant homoeostasis was affected suggesting that LAMP3 dysfunction might also present with a mild phenotype or even remain asymptomatic. This was further supported by the Israeli study, which reported both symptomatic relatives, from birth to adulthood and asymptomatic relatives, carrying the G288R *LAMP3* variant in the homozygous state.[9] On the contrary, three other patients from two families have very recently been reported in an abstract at a medical meeting, all presenting neonatal respiratory distress syndrome with ground glass opacities.[10] The proband reported herein with compound heterozygous *LAMP3* variants, had a delayed presentation of chILD at 9 years. *LAMP3* deficiency appears to manifest heterogeneously with

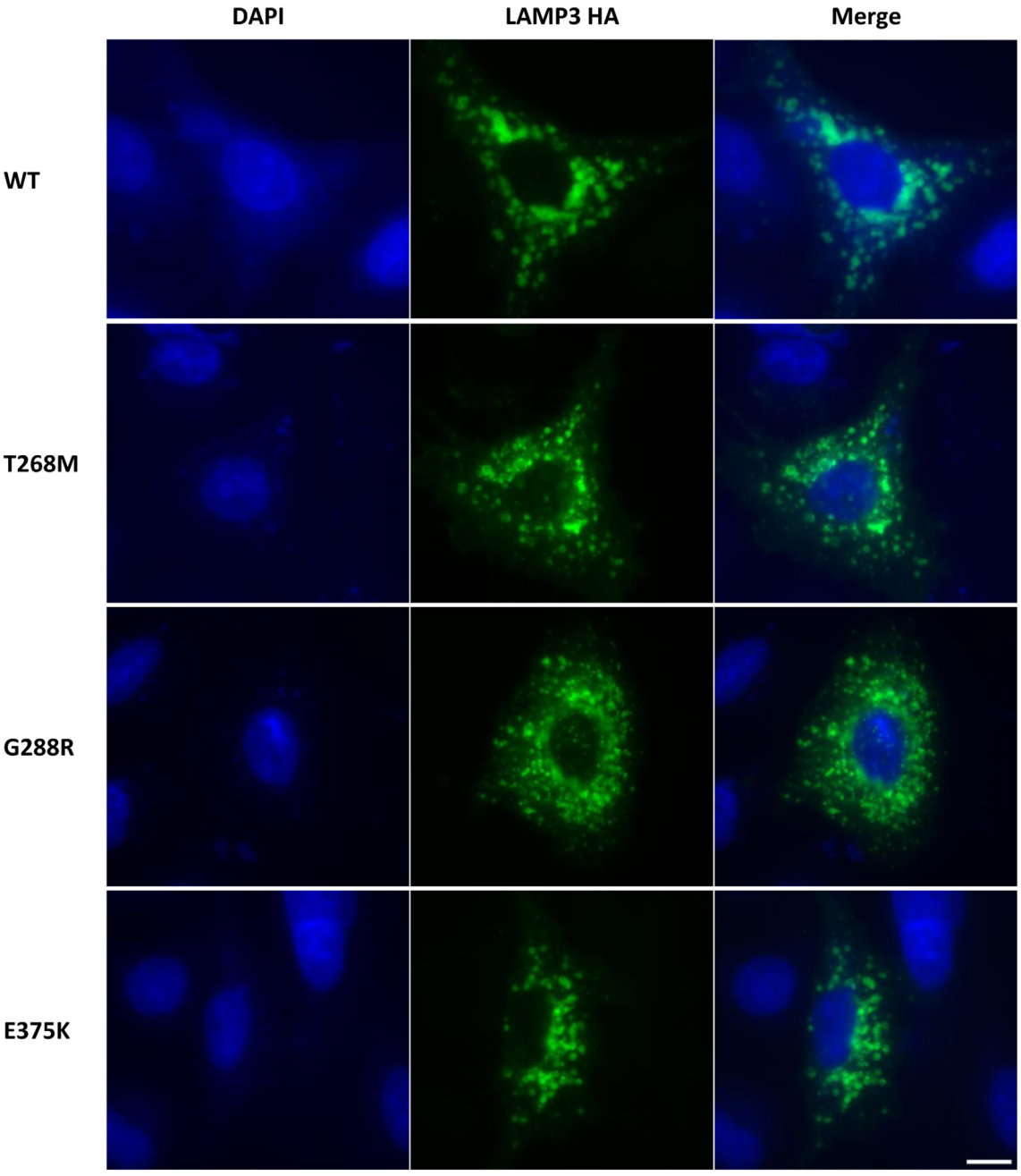

***Fig. 3:* Subcellular localisation of LAMP3**. Immunofluorescence staining of HA-tagged LAMP3 wild-type (WT) and T268M, G288R, and E375K mutant proteins in A549 cells. Scale bar correspond to 10 µm. Results are representative of three independent experiments.

variable ages of onset, whereas most surfactant metabolism disorders usually present clinically at birth or during infancy.[17–19] For example, more than 80% of ABCA3 patients manifest at birth with fatal forms of the disease.[19]

The proband's previous chILD workup did not find a definite cause.[6] Interestingly, no auto-immune markers were detected despite iterative measures.[6,20] Chest CT scan showed severe ILD lesions with ground glass opacities and signs of lung fibrosis despite the young age of the proband. Lung biopsy was also non-specific and could not provide an aetiologic diagnosis. Despite the absence of cysts on CT, lung histology highlighted microcysts, commonly observed in surfactant

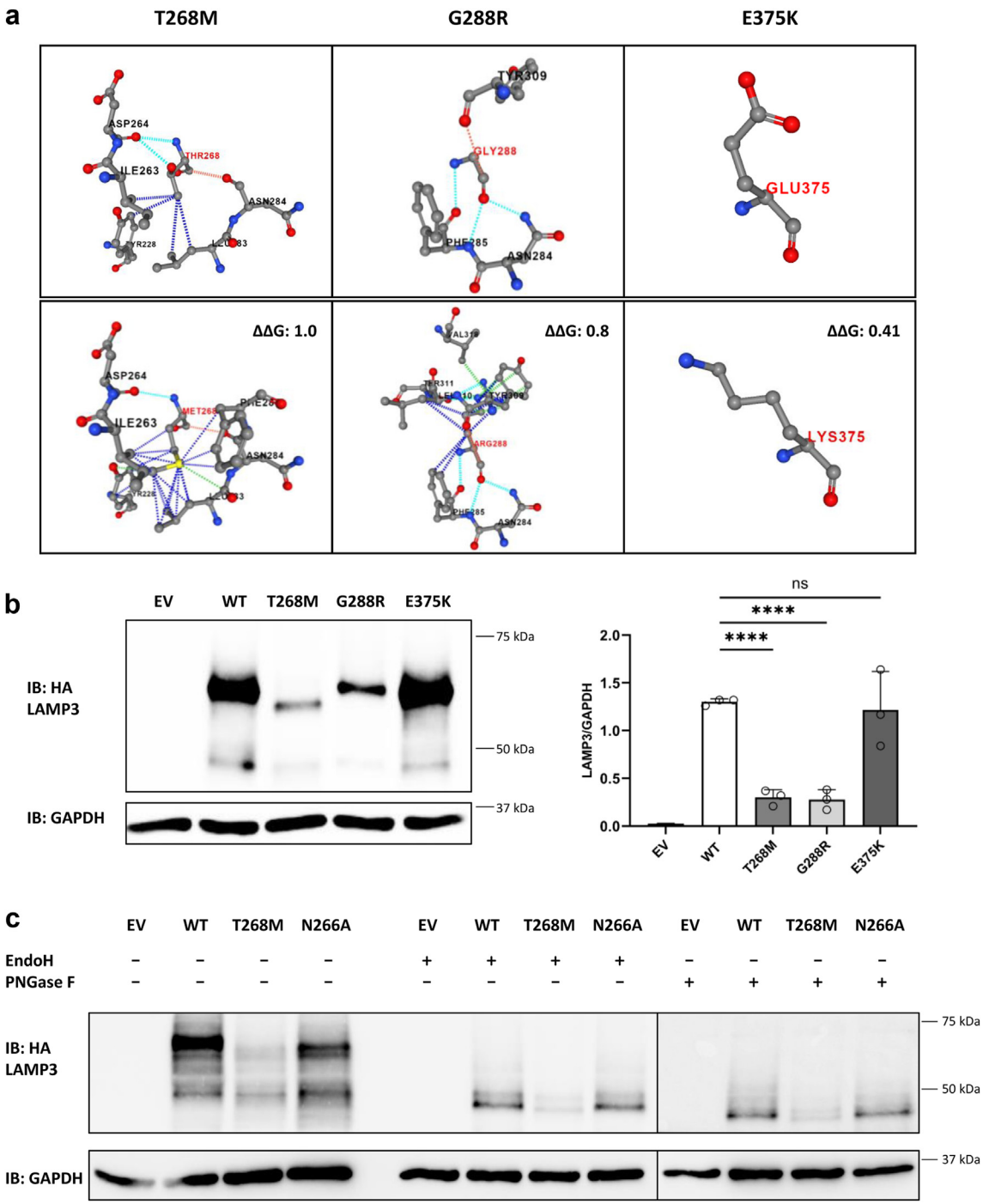

Fig. 4: **Protein stability prediction and protein expression of WT, T268M, G288R, and E375K LAMP3**. **(a)** Impact of the three variants on protein stability based on human LAMP3 crystal structure of the LAMP domain (PDB: 4AKM). An unfolding Gibbs free energy score (ΔΔG) above 0 is predictive of a destabilising effect (PremPS tool). Oxygen atoms are represented in red; nitrogen atoms are represented in blue; the remaining atoms are in grey. Interactions are represented in dotted lines: van der Waals (green), carbonyl (orange), hydrophobic (blue), and polar (cyan). **(b)** Protein expression of HA-tagged LAMP3 WT and mutant proteins from lysate, 48 h after transfection in A549 cells. **(c)** N-glycosylation analysis of HA-tagged LAMP3 WT, T268M, and N266A (as a control for N266 glycosylation loss) performed on protein lysates after digestion with (+) Endo H, PNGase F or without (–) treatment in A549 cells. HA-tagged LAMP3 proteins were fully deglycosylated after Endo H or PNGase F treatments, leading to a shift in electrophoretic mobility to 45–46 kDa. Proteins were detected by immunoblot (IB) using an anti-HA for LAMP3 and anti-GAPDH as a loading control. Protein intensity was quantified by Image J software. Results are representative of three independent experiments. Data are plotted with SD error bars. Unpaired two-tailed Student's t-test was used, p-values < 0.05 were considered statistically significant. ****p < 0.0001 and non significative (ns) p > 0.05.

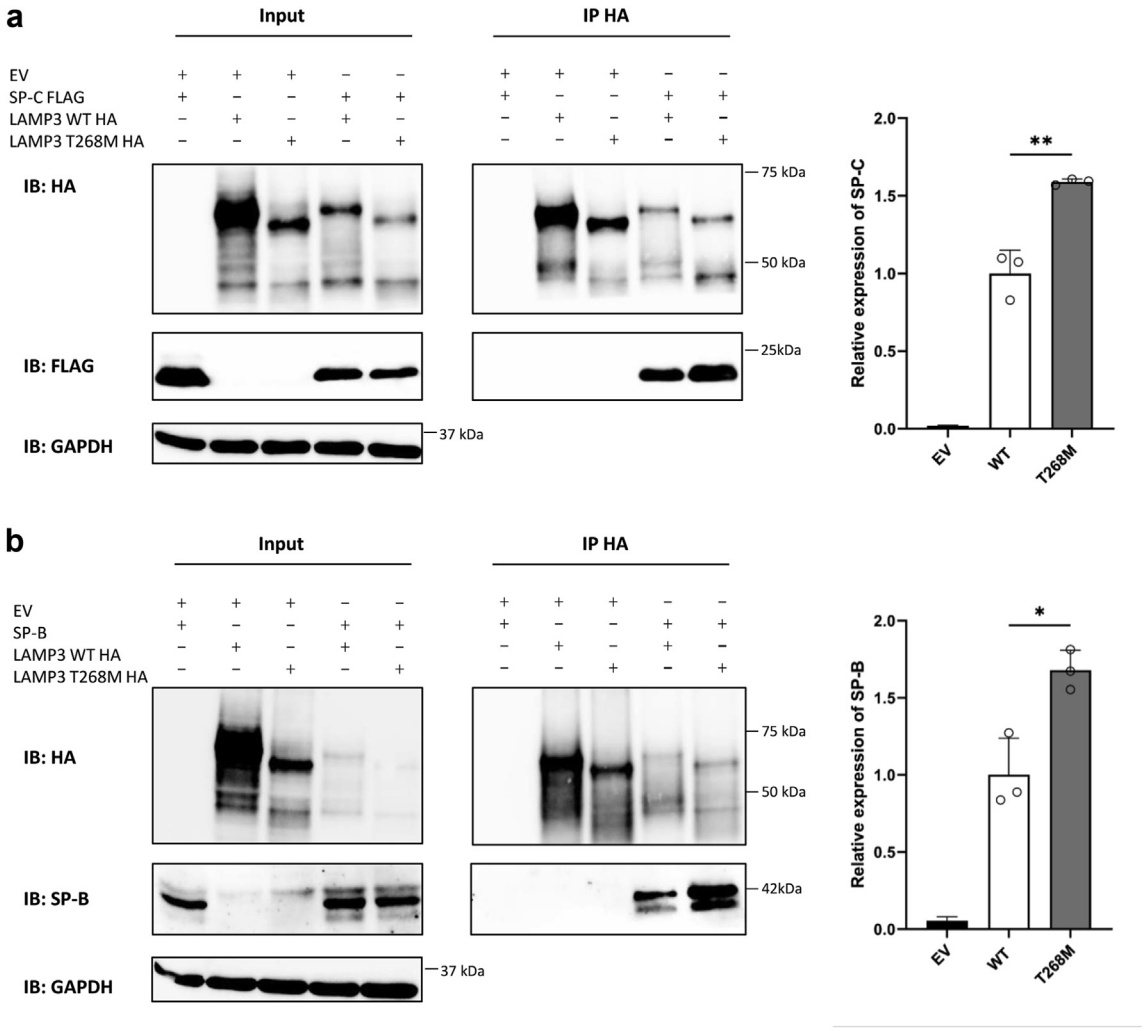

***Fig. 5*: Interaction of LAMP3 and surfactant proteins C (SP-C) and B (SP-B)**. HA-tagged LAMP3 WT or T268M proteins were co-expressed (input) with a empty vector (EV), SP-C FLAG **(a)** or SP-B **(b)** and immunoprecipitated (IP) with an anti-HA antibody in A549 cells. Proteins were detected by immunoblot (IB) using an anti-HA antibody for LAMP3, an anti-FLAG antibody for SP-C, an anti-proSP-B antibody for SP-B. GAPDH was used as a loading control. Protein intensity was quantified by Image J software. Results are representative of three independent experiments. Data are plotted with SD error bars. Co-IP levels of SP-C **(a)** and SP-B **(b)** with EV, LAMP3 WT and LAMP3 T268M were quantified and normalised with LAMP3 WT. Unpaired two-tailed Student's t-test was used. p-values < 0.05 were considered statistically significant. p-values <0.05 and <0.01 are indicated with * and **, respectively.

disorders.[18,21–24] A notable challenge in the clinical characterisation of the proband is the presence of comorbidities that do not appear to be attributable to his *LAMP3* deficiency. A proportion of these appear to be attributable to 21-hydroxylase deficiency (e.g., growth retardation, micropenis and bilateral cryptorchidism).

The functional consequences of the two *LAMP3* variants Y302Qfs*2 and T268M identified in the proband were then functionally characterised. The loss-of-function effect of these two variants was demonstrated *ex vivo* at the mRNA and protein levels in proband lung tissue and nasal epithelial cells and *in vitro* after transient overexpression of recombinant *LAMP3* in A549 cells. In addition, the deleterious effect of the G288R variant identified in a large consanguineous family with inherited chILD reported by Rips et al.[9] was also assessed.

The two missense variants T268M and G288R identified in the proband and the Israeli pedigree, respectively, are located in the LAMP domain of the protein, near a cysteine involved in the first disulfide bond. Both missense variants change the polarity of the amino acid and are predicted to change local intramolecular interactions. A significant reduction of

protein expression was shown *in vitro* for these two variants. In addition, we demonstrated that the T268M-LAMP3 protein has a shorter half-life than the WT. In contrast, the human equivalent of the missense variant identified in AT dogs, E375K, did not alter protein expression. The E375K variant, also located in the LAMP domain, was predicted *in silico* to moderately impair the protein stability. However, the method used to quantify LAMP3 (i.e., Western blot) may not have detected a more subtle effect on protein stability.

Besides decreasing LAMP3 expression, we have demonstrated that the missense variant T268M also disturbs the N-glycosylation of asparagine 266. N-glycosylation is a crucial post-translational modification that can impact protein stability through appropriate folding and/or trafficking. In the case of the LAMP3-N266A used as a negative control of glycosylation, the substitution of asparagine 266 by an alanine did not appear to impair the stability of the protein, suggesting that N266A might not be as destabilising as the T268M. In other LAMP family members, it has been shown that the removal of N-glycans by Endo H treatment in LAMP1 and in LAMP2 resulted in more rapid degradation of the proteins while the lysosomes containing these proteins remained stable,[12] thus indicating that N-glycans protect against acidic proteases. An immunofluorescence study revealed that the T268M mutant did not disturb LAMP3 subcellular localisation, and it may be hypothesised that only one disturbed glycosylation site may not fully impair the protein trafficking or affect organelle stability.

The exact function of LAMP3 remains unclear. LAMP3 expression is restricted to dentritic cells and AEC2.[13] Recently, overexpression of LAMP3 in salivary gland epithelial cells was shown to inhibit autophagy, leading to apoptosis in patients with Sjögren's syndrome.[25] In AEC2, several elements point to a crucial role in surfactant metabolism. First, *LAMP3* expression is regulated by the thyroid transcripton factor-1 (TTF-1, also called NKX2-1) that also regulates surfactant related genes: *SFTPB, SFTPC, ABCA3, SFTPA1,* and *SFTPA2*.[26,27] Second, in dogs presenting with fatal neonatal respiratory distress and homozygous for the *LAMP3* missense E387K LAMP3 variant, abnormal LBs were also found.[7] Additionally, in another study, *Lamp3*$^{-/-}$ mice showed increased levels of proSP-C and mature SP-B with abnormal LB formation.[8] In the present study, we demonstrated *in vitro* by co-immunoprecipitation an interaction between LAMP3 and the two surfactant proteins SP-B and SP-C. Moreover, the study of the LAMP3 T268M protein revealed an increase of pro-SP-C and pro-SP-B interaction levels as compared to the WT form of the protein, reflecting that LAMP3 dysfunction may alter surfactant homoeostasis. Finally, the decrease in proSP-B and SP-B levels observed in the patient's lung biopsy supports the involvement of LAMP3 in SP-B metabolism.

In conclusion, *LAMP3* dysfunction emerges as a molecular cause of chILD, impairing surfactant metabolism. The heterogeneous phenotypes in humans, mice, and dog models illustrate that the phenotype of *LAMP3* dysfunction deserves to be further characterised. The characteristic high-resolution chest CT scan and histological ILD patterns of patients with *LAMP3* deficiency support the inclusion of *LAMP3* sequencing in the genetic work-up of both children and adults with ILD.[1,6]

Contributors

Conceptualisation: CL, TD, and NN.

Investigation and data collection, including accessing and verifying the underlying data: CL, TD, YS, MDR, LT, VN, FDLM, ACLH, and NN.

Histological analysis: ACLH.

Supervision: CL and NN.

Writing original draft: CL, TD, and NN.

Writing review & editing: CL, TD, YS, MDR, LT, JAB, FSC, MD, AF, MG, DH, LK, CM, HM, JR, JAW, DJW, SA, ML, IG, SAK, OB, ACLH, and NN.

All authors read and approved the final version of the manuscript.

Data sharing statement

The datasets generated and/or analysed during the current study are available in the Supplemental Material of this article and upon request. This includes raw data, processed data, and any additional materials necessary to replicate the study findings. For any further enquiries or requests, please contact the corresponding author.

Declaration of interests

TD declares a grant from RespiFil for participation in the ERS congress, and a short-term scientific mission by the COST Innovators Grant CIG16125 2022; MG declares a grant from DFG Gr970/9-2; NN declares grants from the French Ministry of Health, Million Dollar Bike Ride, Chancellerie des Universités, RespiFIL, payment for writing the manuscript by La lettre du Pneumologue and support for attending meetings from the ERS. The other authors declare no conflicts of interest.

Acknowledgements

We are grateful to the patient and his family, whose cooperation made this study possible. We thank the national networks for rare lung diseases: Centre de référence des maladies respiratoires rares (RespiRare), the US National Institutes of Health (NIH) and the Children's Discovery Institute.

Appendix A. Supplementary data

Supplementary data related to this article can be found at https://doi.org/10.1016/j.ebiom.2025.105626.

References

1 Bush A, Cunningham S, de Blic J, et al. European protocols for the diagnosis and initial treatment of interstitial lung disease in children. *Thorax*. 2015;70(11):1078–1084. https://doi.org/10.1136/thoraxjnl-2015-207349.

2 Kurland G, Deterding RR, Hagood JS, et al. An official American Thoracic Society clinical practice guideline: classification, evaluation, and management of childhood interstitial lung disease in infancy. *Am J Respir Crit Care Med*. 2013;188(3):376–394. https://doi.org/10.1164/rccm.201305-0923ST.

3 Laenger FP, Schwerk N, Dingemann J, et al. Interstitial lung disease in infancy and early childhood: a clinicopathological primer. *Eur Respir Rev*. 2022;31(163):210251. https://doi.org/10.1183/16000617.0251-2021.

4 Torrent-Vernetta A, Gaboli M, Castillo-Corullón S, et al. Incidence and prevalence of Children's diffuse lung disease in Spain. *Arch Bronconeumol*. 2022;58(1):22–29. https://doi.org/10.1016/j.arbres.2021.06.001.

5 Fletcher C, Hadchouel A, Thumerelle C, et al. Epidemiology of childhood interstitial lung disease in France: the RespiRare cohort. *Thorax*. 2024;79(9):842–852. https://doi.org/10.1136/thorax-2023-221325. Published online July 4, 2024:thorax-2023-221325.

6 Nathan N, Griese M, Michel K, et al. Diagnostic workup of childhood interstitial lung disease. *Eur Respir Rev*. 2023;32(167):220188. https://doi.org/10.1183/16000617.0188-2022.

7 Dillard KJ, Ochs M, Niskanen JE, et al. Recessive missense LAMP3 variant associated with defect in lamellar body biogenesis and fatal neonatal interstitial lung disease in dogs. *PLoS Genet*. 2020;16(3):e1008651. https://doi.org/10.1371/journal.pgen.1008651.

8 Lunding LP, Krause D, Stichtenoth G, et al. LAMP3 deficiency affects surfactant homeostasis in mice. *PLoS Genet*. 2021;17(6):e1009619. https://doi.org/10.1371/journal.pgen.1009619.

9 Rips J, Halstuk O, Fuchs A, et al. Unbiased phenotype and genotype matching maximizes gene discovery and diagnostic yield. *Genet Med*. 2024;26(4):101068. https://doi.org/10.1016/j.gim.2024.101068.

10 Hinds D, Keehan L, Fischer AJ, et al. Bi-Allelic LAMP3 variants in three children with interstitial lung disease: evidence of a novel disease-gene association. In: *D28. PEDIATRIC PULMONOLOGY BENCH-TO-BEDSIDE: GENETICS, WHOLE-EXOME SEQUENCING, AND OMICS. American Thoracic Society International Conference Abstracts*. American Thoracic Society; 2024:A7155. https://doi.org/10.1164/ajrccm-conference.2024.209.1_MeetingAbstracts.A7155.

11 Eskelinen EL. Roles of LAMP-1 and LAMP-2 in lysosome biogenesis and autophagy. *Mol Aspects Med*. 2006;27(5–6):495–502. https://doi.org/10.1016/j.mam.2006.08.005.

12 Wilke S, Krausze J, Büssow K. Crystal structure of the conserved domain of the DC lysosomal associated membrane protein: implications for the lysosomal glycocalyx. *BMC Biol*. 2012;10:62. https://doi.org/10.1186/1741-7007-10-62.

13 Salaun B, de Saint-Vis B, Pacheco N, et al. CD208/dendritic cell-lysosomal associated membrane protein is a marker of normal and transformed type II pneumocytes. *Am J Pathol*. 2004;164(3):861–871. https://doi.org/10.1016/S0002-9440(10)63174-4.

14 Zhao M, Venosa A, Tomer Y, Beers MF, Mulugeta S. Cell type- and protein-specific induction of LAMP3. *FASEB J*. 2019;33(S1):462–464. https://doi.org/10.1096/fasebj.2019.33.1_supplement.462.4.

15 Wade KC, Guttentag SH, Gonzales LW, et al. Gene induction during differentiation of human pulmonary type II cells in vitro. *Am J Respir Cell Mol Biol*. 2006;34(6):727–737. https://doi.org/10.1165/rcmb.2004-0389OC.

16 Chen Y, Lu H, Zhang N, Zhu Z, Wang S, Li M. PremPS: predicting the impact of missense mutations on protein stability. *PLoS Comput Biol*. 2020;16(12):e1008543. https://doi.org/10.1371/journal.pcbi.1008543.

17 Nogee LM, Wert SE, Proffit SA, Hull WM, Whitsett JA. Allelic heterogeneity in hereditary surfactant protein B (SP-B) deficiency. *Am J Respir Crit Care Med*. 2000;161(3):973–981. https://doi.org/10.1164/ajrccm.161.3.9903153.

18 Guillot L, Epaud R, Thouvenin G, et al. New surfactant protein C gene mutations associated with diffuse lung disease. *J Med Genet*. 2009;46(7):490–494.

19 Wambach JA, Casey AM, Fishman MP, et al. Genotype-phenotype correlations for infants and children with ABCA3 deficiency. *Am J Respir Crit Care Med*. 2014;189(12):1538–1543. https://doi.org/10.1164/rccm.201402-0342OC.

20 Falhammar H, Frisén L, Hirschberg AL, Nordenskjöld A, Almqvist C, Nordenström A. Increased risk of autoimmune disorders in 21-hydroxylase deficiency: a Swedish population-based national cohort study. *J Endocr Soc*. 2019;3(5):1039–1052. https://doi.org/10.1210/js.2019-00122.

21 Semple TR, Ashworth MT, Owens CM. Interstitial lung disease in children made easier…well, almost. *Radiographics*. 2017;37(6):1679–1703. https://doi.org/10.1148/rg.2017170006.

22 Semple T, Winant AJ, Lee EY. Childhood interstitial lung disease: imaging guidelines and recommendations. *Radiol Clin*. 2022;60(1):83–111. https://doi.org/10.1016/j.rcl.2021.08.009.

23 Manali ED, Legendre M, Nathan N, et al. Bi-allelic missense ABCA3 mutations in a patient with childhood ILD who reached adulthood. *ERJ Open Res*. 2019;5(3). https://doi.org/10.1183/23120541.00066-2019.

24 Flamein F, Riffault L, Muselet-Charlier C, et al. Molecular and cellular characteristics of ABCA3 mutations associated with diffuse parenchymal lung diseases in children. *Hum Mol Genet*. 2012;21(4):765–775.

25 Tanaka T, Warner BM, Michael DG, et al. LAMP3 inhibits autophagy and contributes to cell death by lysosomal membrane permeabilization. *Autophagy*. 2022;18(7):1629–1647. https://doi.org/10.1080/15548627.2021.1995150.

26 Stuart WD, Fink-Baldauf IM, Tomoshige K, Guo M, Maeda Y. CRISPRi-mediated functional analysis of NKX2-1-binding sites in the lung. *Commun Biol*. 2021;4(1):568. https://doi.org/10.1038/s42003-021-02083-4.

27 Kolla V, Gonzales LW, Gonzales J, et al. Thyroid transcription factor in differentiating type II cells: regulation, isoforms, and target genes. *Am J Respir Cell Mol Biol*. 2007;36(2):213–225. https://doi.org/10.1165/rcmb.2006-0207OC.